Octupole correlations in U and Pu nuclei

N. V. Zamfir[1,2,3] and Dimitri Kusnezov[4]
[1]*Wright Nuclear Structure Laboratory, Yale University, New Haven, Connecticut 06520-8124*
[2]*Clark University, Worcester, Massachusetts 01610*
[3]*National Institute for Physics and Nuclear Engineering, Bucharest-Magurele, Romania*
[4]*Center for Theoretical Physics, Sloane Physics Laboratory, Yale University, New Haven, Connecticut 06520-8120*
(Received 11 September 2002; published 17 January 2003)

We study the even-even U and Pu nuclei in the framework of the $spdf$ interacting boson model. Analysis of the systematics of positive and negative parity bands, together with the $E1$, $E2$, and $E3$ transitions, suggests that the properties of low-lying states can be understood without the introduction of stable octupole deformation. Double octupole phonon characteristics are also identified in certain low-lying 0^+ excited states in U and Pu.

DOI: 10.1103/PhysRevC.67.014305 PACS number(s): 21.60.Fw, 21.10.Re, 23.20.Lv, 27.90.+b

I. INTRODUCTION

Octupole correlations in the actinides have attracted interest since the predictions that octupole deformation would be present in the $Z\sim 88$ and $N\sim 134$ region [1]. These predictions have been explored through a series of experimental studies, which have centered on energy spectra and transition properties [2]. Numerous theoretical studies were dedicated over the years to the octupole degree of freedom in nuclei [2,3]. A suitable and versatile model for the description of quadrupole-octupole collective degrees of freedom in even-even nuclei is the interacting boson model (IBM) [4]. Recently, an extensive study of the collective negative parity states in the even-even Ra-Th nuclei was completed [5] in the framework of the $spdf$ IBM [6]. In that study, a consistent picture was obtained over the entire nuclear region of the light actinides using a minimal Hamiltonian. The aim of this work is to extend that analysis to U and Pu nuclei, providing a consistent view of the systematics of the even and odd parity states from $Z=86$ to $Z=94$.

We will examine the full systematics of all available data on energies and electromagnetic transitions. The data are from Refs. [7–19]. The full $spdf$ IBM Hamiltonian contains over 50 interaction terms, however, simple physical considerations can reduce the form of the Hamiltonian H [20]. We will use a four parameter model for H, which includes a single quadrupole strength and three boson single particle energies. The form of the Hamiltonian and transition operators are further constrained by the recent analysis of the Rn, Ra, and Th nuclei. We would like to see whether octupole deformation is an essential ingredient in the understanding of the nuclei in this mass region.

II. *spdf* INTERACTING BOSON MODEL

The interacting boson model offers a phenomenological approach of collective nuclear structure by introducing bosons of a given spin, which are associated with the corresponding multipole modes. The quadrupole vibrations and deformations are described in terms of interacting s and d bosons with $L^\pi=0^+$ and $L^\pi=2^+$, respectively. Negative parity states are described by introducing bosons with odd values of angular momentum. In the sdf model, only $f(L^\pi=3^-)$ bosons are used [4,21,22], while in the $spdf$ model, both f and $p(L^\pi=1^-)$ bosons are included (see, for example, Ref. [5], and references therein). The $spdf$ is the preferred model since it is closer in spirit to the sd IBM, including the same dynamical symmetry limits as well as the possibility of octupole deformation.

We are interested in studying the behavior of negative parity states in a region of large quadrupole deformation very close to the $\mathrm{SU}_{sd}(3)$ limit. This requires a minimal Hamiltonian to include a vibrational contribution and a quadrupole interaction. The simplest form of such a Hamiltonian for positive parity states is $H=\epsilon_d\hat{n}_d-\kappa\hat{Q}_{sd}\cdot\hat{Q}_{sd}$. The natural extension of this Hamiltonian to describe both positive and negative parity states simultaneously is realized in the $spdf$ model as

$$H=\epsilon_d\hat{n}_d+\epsilon_p\hat{n}_p+\epsilon_f\hat{n}_f-\kappa\hat{Q}_{spdf}\cdot\hat{Q}_{spdf}, \tag{1}$$

where ϵ_p, ϵ_d, and ϵ_f are the boson energies and $\hat{n}_p$, $\hat{n}_d$, and $\hat{n}_f$ are the boson number operators. This is the same Hamiltonian used to describe the transitional actinides in Ref. [5]. The $spdf$ model space admits a $\mathrm{SU}_{spdf}(3)$ limit which is the natural extension of the $\mathrm{SU}_{sd}(3)$ limit of the sd IBM. In the $spdf$ model, the quadrupole operator is given by

$$\hat{Q}_{spdf}=\hat{Q}_{sd}+\hat{Q}_{pf}=[s^\dagger\tilde{d}+d^\dagger s]-\frac{\sqrt{7}}{2}[d^\dagger\tilde{d}]^{(2)}+\frac{3\sqrt{7}}{5}\times[p^\dagger\tilde{f}+f^\dagger\tilde{p}]^{(2)}-\frac{9\sqrt{3}}{10}[p^\dagger\tilde{p}]^{(2)}-\frac{3\sqrt{42}}{10}[f^\dagger\tilde{f}]^{(2)}. \tag{2}$$

This is related to the Casimir operator of the $\mathrm{SU}_{spdf}(3)$ subgroup. Note that the same strength κ of the quadrupole interaction describes the sd bosons and the pf bosons.

The transition operators $T(E1)$, $T(E2)$, and $T(E3)$ are not all defined from dynamical symmetry considerations, so

that there is some freedom in their form. We will take all these operators to be one-body operators. While the $T(E2)$ operator has five terms, we use the quadrupole operator above, which fixes the parameters, aside from the effective charge:

$$T(E2)=e_2\hat{Q}_{spdf}. \tag{3}$$

$E1$ transitions are studied using the three term, one-body operator:

$$T^{(E1)}_{spdf}=e_1([p^\dagger\tilde{d}+d^\dagger\tilde{p}]^{(1)}+\chi^{(1)}_{sp}[s^\dagger\tilde{p}+p^\dagger s]^{(1)} +\chi^{(1)}_{df}[d^\dagger\tilde{f}+f^\dagger\tilde{d}]^{(1)}) \tag{4}$$

and similarly, the $E3$ operator is

$$T^{(E3)}_{spdf}=e_3([d^\dagger\tilde{f}+f^\dagger\tilde{d}]^{(3)}+\chi^{(3)}_{pd}[p^\dagger\tilde{d}+d^\dagger\tilde{p}]^{(3)} +\chi^{(3)}_{sf}[s^\dagger\tilde{f}+f^\dagger s]^{(3)}). \tag{5}$$

Since we are interested in the global systematics of the actinides, the recent study of $Z=86$–90 nuclei will constrain these transition operator parameters. For the $E1$ and $E3$, we will further attempt to use the minimal number of terms when possible, consistent with the lighter actinides. In this study, the parametrization is kept as simple as possible and no attempt of fine tuning is made.

The calculations are done with the code OCTUPOLE [23]. The total boson numbers N_B are calculated in the usual way, except that the neutron boson numbers are counted relative to $N=164$, which was proposed [24] to be a spherical subshell closure, in addition to the major shell closures at $N=126$ and 184. To simplify the numerical diagonalizations, we will use a truncated basis allowing only one pf boson ($N_{pf}=1$). We will verify that for the parameter choices below, this is a good approximation of the full space calculations for the low-energy states. Extending the basis, by allowing up to three pf bosons ($N_{pf}=3$), the predicted properties of the states discussed here remain practically unchanged. The only exception is the appearance of an additional low-lying $K=0^+$ excitation, which has a double octupole phonon character. The comparison of the truncation to the full calculations has already been examined in Ref. [5] for this Hamiltonian.

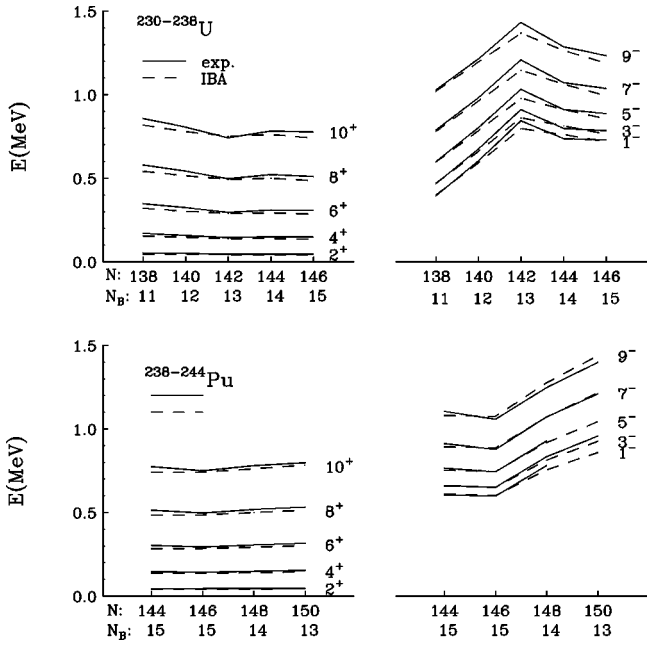

FIG. 1. Experimental (continuous lines) and calculated (dashed lines) energies for the $K^\pi=0^+_1,0^-_1$ bands in $^{230-238}$U and $^{238-244}$Pu.

III. DISCUSSION

A. Energy spectra

Consider first the experimental $K^\pi=0^+_1$ and $K^\pi=0^-_1$ bands in U and Pu. These are shown in Fig. 1 (solid lines). One can see an interesting structural change near $N=142$ in U and near $N=146$ in Pu. Unfortunately, there is no data in U beyond $N=146$ or Pu near $N=142$ to see if analogous structural changes are present in each isotopic chain. The minimum observed in the negative parity states at $N=146$ in Pu and possibly in U has been interpreted as an evidence for increased octupole correlations [25]. What is more striking in this figure, is the correlation of the structural changes in the negative parity states with subtle changes in the positive parity states. This effect is not readily seen in the 2^+ state systematics. One must go to higher spin, such as 10^+, to see the effect. A second minimum can be seen in the U isotopic chain, where the energy is rapidly decreasing with the decreasing neutron number towards $N=132$. (Such a minimum is seen in the Ra and Th isotopes [5].) This is in agreement with the prediction that the lowest octupole excitation should be in $^{224}U_{132}$ which is, supposedly, the most octupole deformed nucleus in its ground state [2].

In Fig. 1, we also present the $spdf$ IBM calculations (dashed) for the $K^\pi=0^+_1$ and $K^\pi=0^-_1$ bands. Of the four Hamiltonian parameters, ϵ_d and κ are essentially constant,

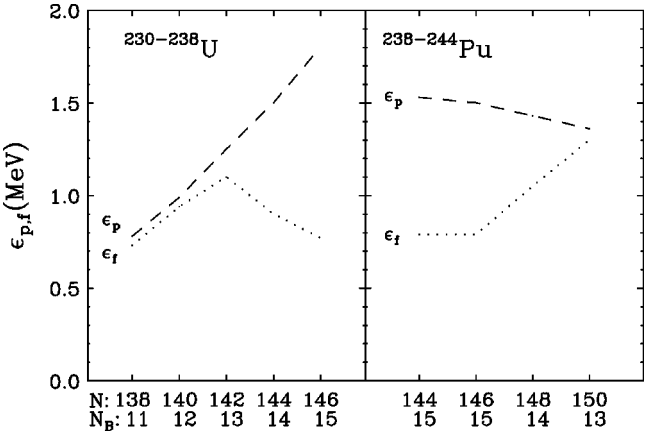

FIG. 2. The energy of the p and f bosons ($\epsilon_{p,f}$) used in the present calculations.

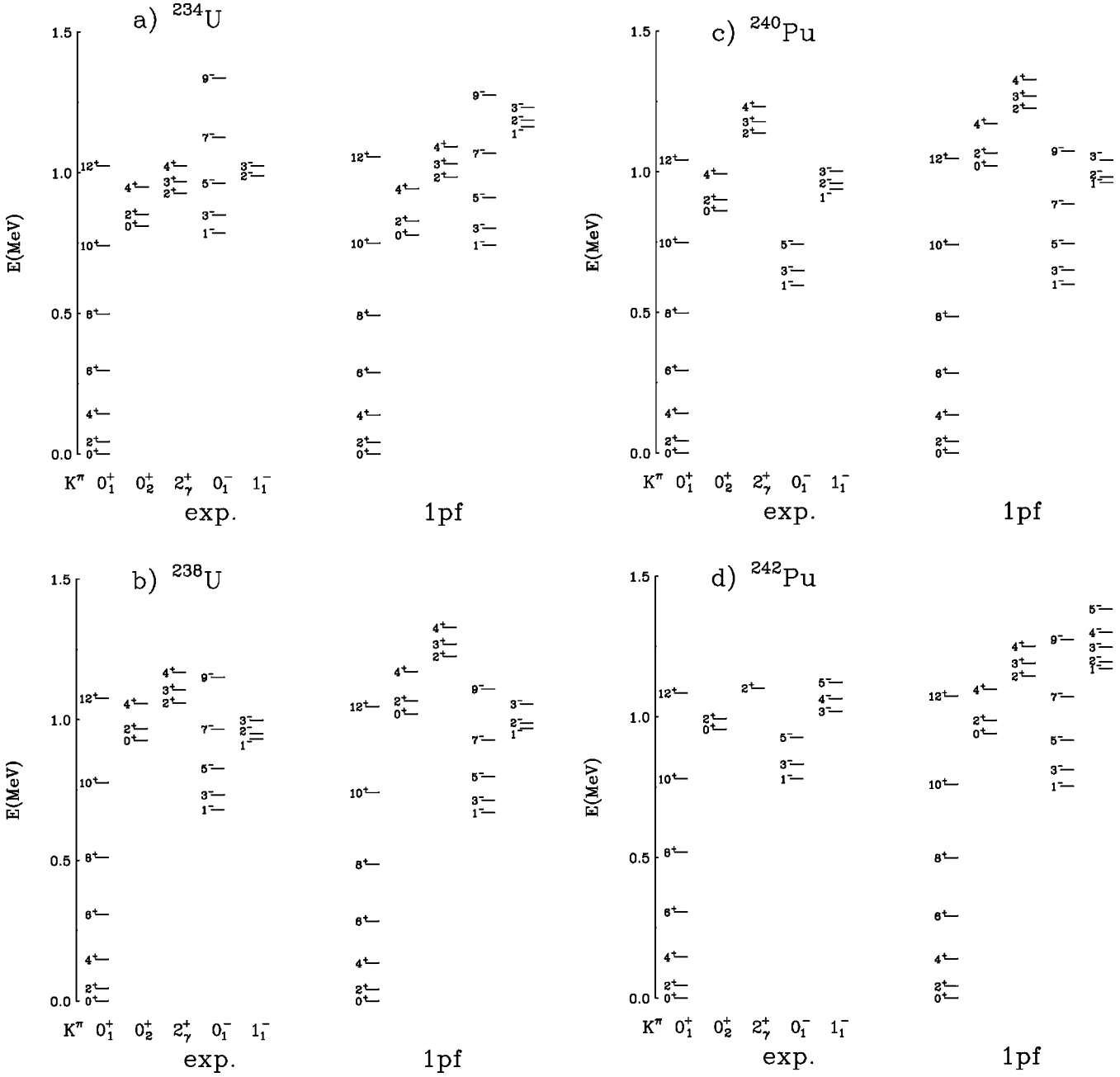

FIG. 3. Comparison of experimental band structure in ^{234,238}U and ^{240,242}Pu with $N_{pf}=1$ calculations.

since these are determined from the positive parity states. We find $\epsilon_d=0.25$ MeV and $\kappa=0.012$ MeV for $N_B=11$–13 and 0.013 MeV for $N_B=14,15$. These values are similar to those in the Ra-Th region [5]. The negative parity states, on the other hand, undergo a more dramatic evolution with boson number. The parameters ϵ_p and ϵ_f, shown in Fig. 2, have a smooth behavior. ϵ_f can be seen to follow the evolution of the excitation energy of the lowest 1^- state. For $N_B \leqslant 13$, we observe that $\epsilon_p \sim \epsilon_f$, a condition which brings the Hamiltonian close to the $SU_{spdf}(3)$ dynamical symmetry limit. In that limit, it is possible to realize low-lying octupole deformation for certain values of the parameters [5]. However, for the present study, such states are not present.

The experimental minimum in excitation energy of the $K=0_1^-$ band at $N=146$ occurs at different energies in U and Pu. In the Hamiltonian, ϵ_d, ϵ_f, and κ have the same values in both nuclei; the difference in energies of this minimum is attributed to ϵ_p, which is larger in U than in Pu.

Beyond the $K=0_1^-$ bands shown in Fig. 1, the experimental situation is not so clear. The next lowest band in ^{236,238}U and ^{238,240}Pu is $K=1^-$. In ^{230}U and ^{244}Pu, no data are available. In ^{232,234}U, the next lowest band is claimed to be $K=2^-$ [8,9], while in ^{242}Pu, it is claimed to be $K=3^-$ [12]. In contrast, in our calculations, the next lowest band is $K=1^-$ for all U and Pu isotopes in this study. Based on the experimental systematics, and on the IBM results, we suggest that

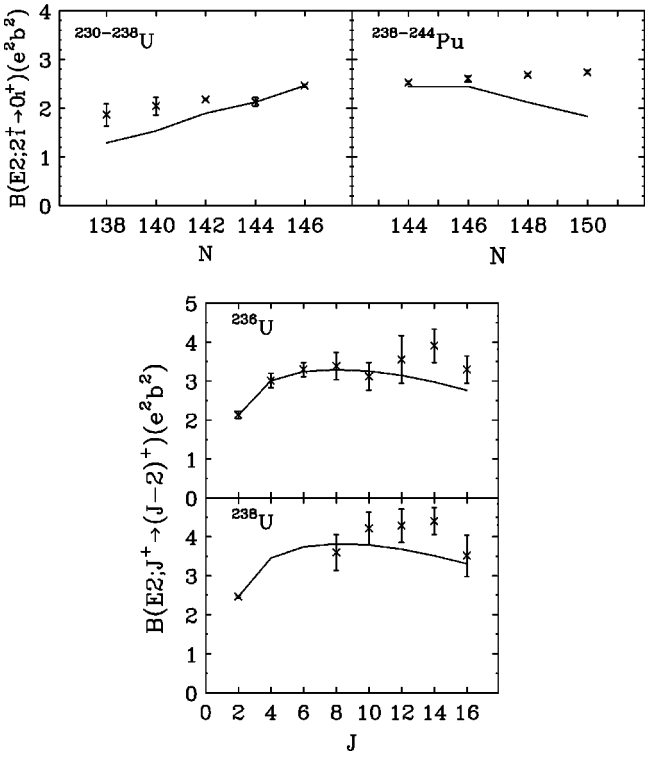

FIG. 4. Comparison of the experimental yrast $B(E2)$ values (symbols) with $N_{pf}=1$ IBM calculations (continuous line). The $E2$ operator is given in Eq. (3) and the effective charge $e_2=0.16$ e b.

those $K=2^-$ and $K=3^-$ bands are in fact $K=1^-$ bands, with the lowest states experimentally missing. In Fig. 3, we show detailed comparisons of the experimental level schemes of ^{234,238}U and ^{240,242}Pu with the calculations. These are representative of all the isotopes studied. The overall agreement is quite good. The yrast bands $K=0_1^+$ and $K=0_1^-$ and the first excited $K=0^+$ and $K=1^-$ bands are reproduced very well, but the γ band $K=2_1^+$ is typically predicted to be 0.1–0.2 MeV higher. A slightly different form of $\hat{Q}_{sd}$ [χ_{sd} lower than $-\sqrt{7}/2$ in Eq. (2)] could be used to improve the agreement. However, for simplicity, we have taken this to be fixed at its $SU_{sd}(3)$ value.

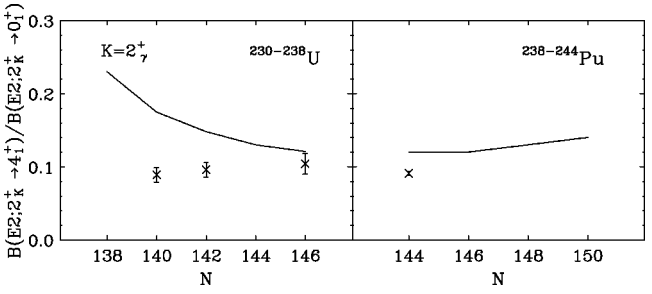

FIG. 5. Comparison of the experimental $B(E2)$ branching ratios (symbols) from the 2_γ^+ state with the $N_{pf}=1$ IBM calculations (continuous lines).

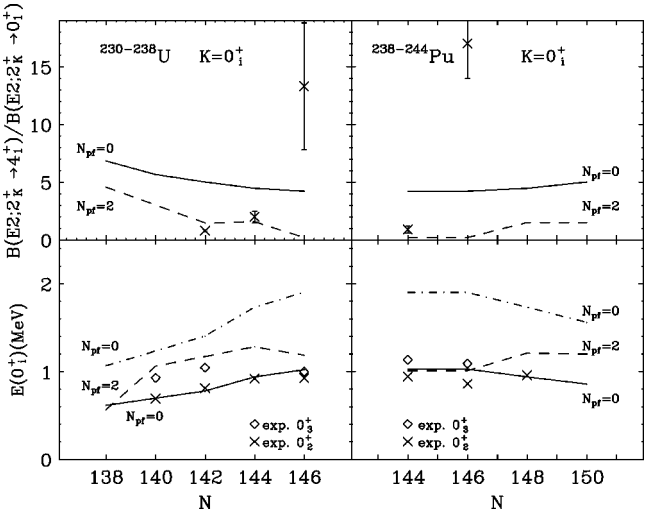

FIG. 6. The excitation energy and the $B(E2)$ branching ratios of the first excited 0^+ states compared with $N_{pf}=0$ (continuous lines, $K=0_2^+$; dot-dashed lines, $K=0_3^+$) and N_{pf} up to 2 (dashed lines: the $K=0^+$ band with $N_{pf}=2$ character, which, depending on the parameter set, is $K=0_2^+$ or 0_3^+ band). A small dipole-dipole interaction is included in the Hamiltonian to produce nonzero $B(E2)$ transition strengths from the $K=0^+$ band based primarily on $N_{pf}=2$ components in the ground state band.

B. Electromagnetic transitions

The experimental situation for transitions is quite good. There are many measurements of absolute $B(E2)$ and $B(E3)$ transitions as well as some selected $B(E1)$ rates. This provides a more stringent test on the wave functions obtained above.

$B(E2;2_1^+\rightarrow 0_1^+)$ transition rates for all the U and Pu isotopes are presented in Fig. 4, together with the $B[E2;J^+\rightarrow(J-2)^+]$ values for the ground state band in ^{236}U and ^{238}U. Using the transition operator (3) leaves one free parameter, the effective charge. The effective charge $e_2=0.16$ e b is taken to be the same for all nuclei. This is similar to the value $e_2=0.18$ e b used in the Ra-Th region. One can see that the transition rates are well described without variation of transition operator parameters. $B(E2)$ branching ratios for the γ bands ($K=2_\gamma^+$) are shown in Fig. 5. We choose the ratio $B(E2;2_\gamma^+\rightarrow 4_1^+)/B(E2;2_\gamma^+\rightarrow 0_1^+)$ for comparison because it does not concern the $2_\gamma^+\rightarrow 2_1^+$ transition, which could introduce unknown $M1$-$E2$ mixing ratios. The agreement is reasonably good. The difference in the trends for U could be accounted for with the same change in $\hat{Q}_{sd}$ discussed above for the γ-band energies.

For the current set of Hamiltonian parameters, there is no difference in the $B(E2)$ transition rates if we use the sd truncation of the $E2$ operator, Q_{sd} or the full $spdf$ form, Q_{spdf}. We have examined the calculations in which $N_{pf}=2$ components are present in the basis states. These combinations of p and f bosons in the positive parity states can contribute to the low-lying wave functions. However, they do not noticeably modify the results we present here. Hence, contributions from possible deformed states are not significant in these observables.

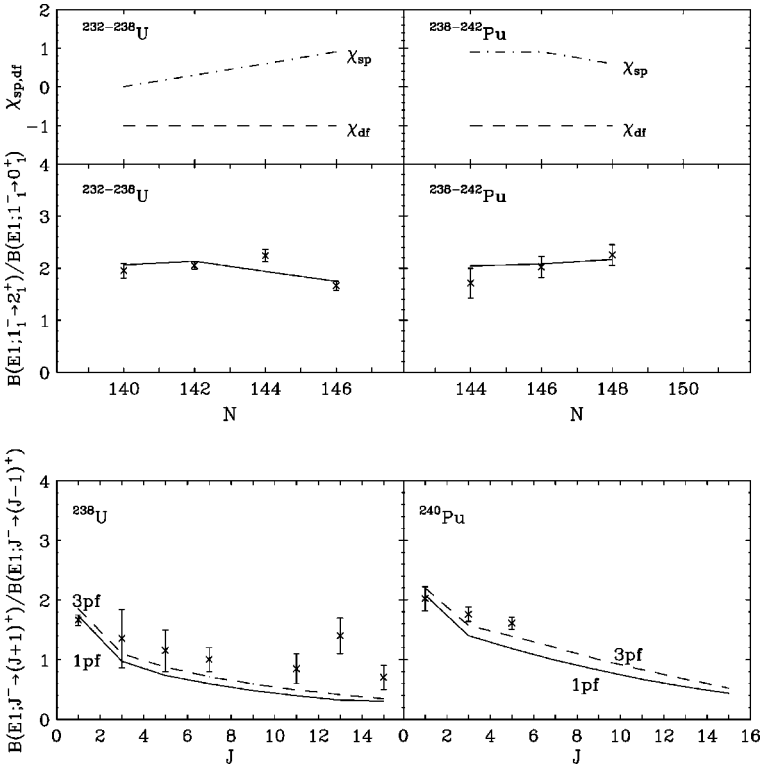

FIG. 7. Top: The parameters $\chi_{sp}^{(1)}$ and $\chi_{df}^{(1)}$ of the $T(E1)$ operator of Eq. (4). Middle: Experimental (symbols) and theoretical (continuous lines) $B(E1)$ branching ratio from 1_1^- states. Bottom: Similar to the middle panels but for $B(E1)$ branching ratios from $J \geqslant 1^-$ states for ^{238}U and ^{240}Pu. The dashed lines show the predictions of the calculations with N_{pf} up to 3.

The corresponding ratio for the decay of the 2^+ member of the $K=0_2^+$ band has an erratic behavior with changes of more than one order of magnitude from one nucleus to the next, despite the smooth evolution of the excitation energy with the boson number N. Figure 6 (top) shows that the IBM calculations predict a ratio of ~ 5. Figure 6 (bottom) shows that they reproduce the excitation energy of the 0_2^+ state reasonably well. However, the 0_3^+ states, where they are known experimentally, are very close in energy to the 0_2^+ states. In contrast, the predicted 0_3^+ states in the $N_{pf}=0$ basis are much higher in energy than the experiment (0.5–1.0 MeV; see Fig. 6 bottom). We will see in the following section that by extending the basis to $N_{pf}=2$ in the positive parity states, the agreement is improved due to the presence of additional octupole two-phonon states.

The $E1$ branching ratios depend only on $\chi_{sp}^{(1)}, \chi_{df}^{(1)}$ and are not dependent on the effective charge e_1. The parameters $\chi_{sp}^{(1)}, \chi_{df}^{(1)}$ which fit the data are presented in Fig. 7 (top). Their values show a smooth evolution, and are similar to those used to describe the transitional actinides [5]. In Fig. 7 (middle) we compare the data and the IBM calculations for the branching ratio $B(E1;1_1^- \rightarrow 2_1^+)/B(E1;1_1^- \rightarrow 0_1^+)$ and in Fig. 7 (bottom) for the branching ratios $B[E1;J^- \rightarrow (J+1)^+]/B[E1;J^- \rightarrow (J-1)^+]$, as a function of spin. The data are from Refs. [8–12,15,16]. In all cases the agreement with the data is excellent. In contrast to the transitional actinides, there is little absolute $B(E1)$ data, so that more precise tests of the $E1$ operator on the A dependence of the effective charge and on the basis (N_{pf}) are not possible. The

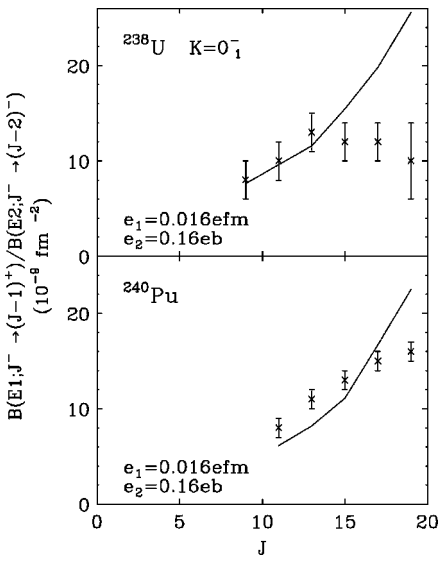

FIG. 8. Experimental $B(E1)/B(E2)$ branching ratios in ^{238}U and ^{240}Pu compared with the predictions of the $N_{pf}=1$ calculations.

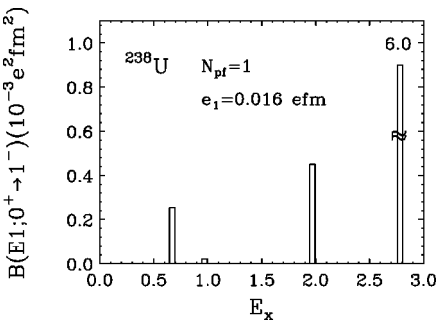

FIG. 9. Theoretical $B(E1;0_1^+ \rightarrow 1^-)$ strength distribution in ^{238}U.

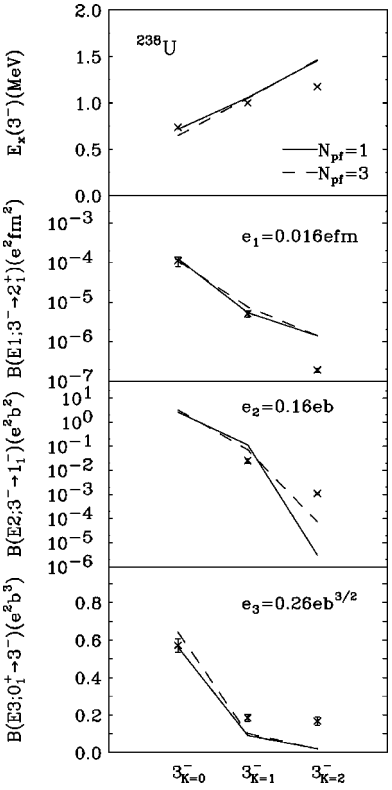

FIG. 10. Comparison of data related to 3_i^- states in ^{238}U with IBM calculations with $N_{pf}=1$ (continuous lines) and N_{pf} up to 3 (dashed lines).

available $E1/E2$ branching ratios are shown in Fig. 8. The spin dependence demonstrates a saturation, which is not reproduced by the calculations.

Using the $E1$ operator effective charge for ^{238}U determined from the $B(E1)/B(E2)$ branching ratios, $e_1=0.016\ e$ fm, leads to the prediction of the absolute $B(E1{:}0_1^+\rightarrow 1_i^-)$ strength in Fig. 9. The strength near 3 MeV is associated with the p boson. In Fig. 10, we compile absolute $B(E1)$, $B(E2)$, and $B(E3)$ data for first three 3^- states in ^{238}U. The parameters for the $E1$ and $E2$ operators have been presented above, while for the $E3$ operator, we use the parameters $e_3=0.26\ e\ \mathrm{b}^{3/2}$, $\chi_{pd}^{(3)}=-1$, and $\chi_{sf}^{(3)}=0$. In general, the agreement is good for the first two 3^- states, $3_{K=0}^-$ and $3_{K=1}^-$, and not so good for the third 3^- state, $3_{K=2}^-$. The data and calculations in the lower panel of Fig. 10 are essentially unchanged for ^{234,236}U, and are not shown. The $E3$ effective charge also provides a reasonable description of the known $B(E3;0_1^+\rightarrow 3_{K=0}^-)$ in the Pu isotopes.

IV. DOUBLE OCTUPOLE/DIPOLE STATES

The comparisons presented in the preceding section show that calculations with $N_{pf}=1$ are able to reproduce the essential features of the $K=0_1^+,0_2^+,2_1^+,0_1^-,1_1^-$, and 2_1^- bands. However, not all excited 0^+ bands are reproduced in the $N_{pf}=1$ calculations presented above (see Fig. 6). In ^{238}U the 0_2^+ and 0_3^+ band heads lie very close in energy: at 926 keV and 997 keV [19,26]. These 0^+ bands are also known in other nuclei studied here: in ^{232}U at 691 keV and 927 keV [8,17], in ^{234}U at 845 keV and 1044 keV [9,17], and in ^{240}Pu the two states appear at 861 and 1089 keV [19]. It was pointed out in Ref. [19] that the two excited bands are widely different in structure. For example, the γ-ray branching ratio $B(E2;2_{0_i}^+\rightarrow 4_1^+)/B(E2;2_{0_i}^+\rightarrow 0_1^+)$ is larger by one order of magnitude for 0_2^+ band as compared with the 0_3^+ band.

It was shown in Ref. [5] that by extending the basis to include more pf bosons, an additional $K=0^+$ excited band based on a $N_{pf}=2$ configuration is predicted at low energy. This type of band corresponds to double octupole/dipole

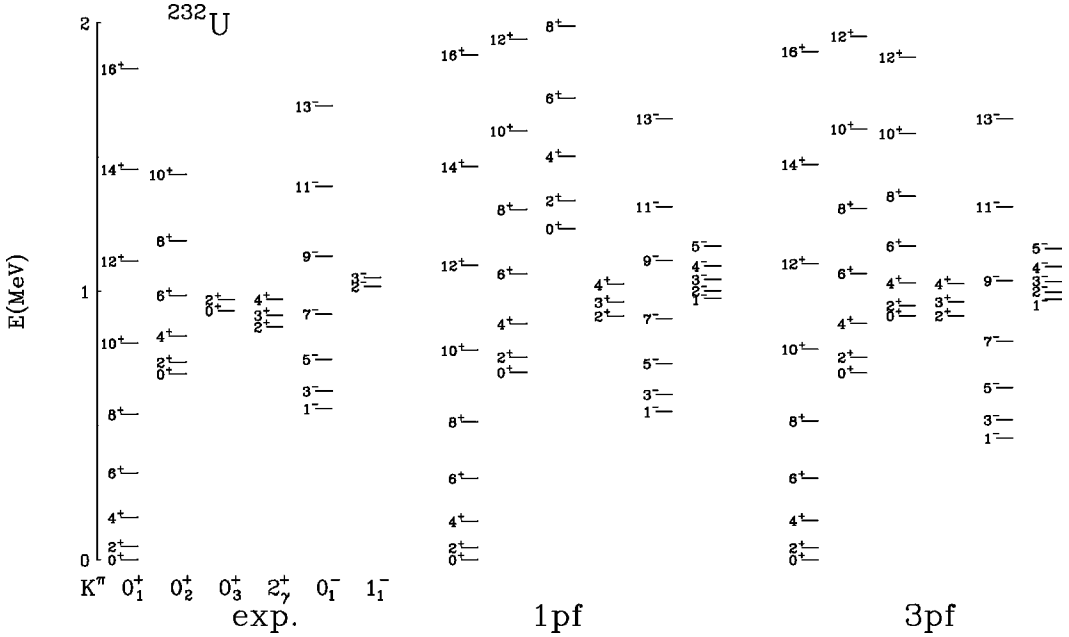

FIG. 11. Comparison of the experimental spectrum of ^{232}U with $N_{pf}=1$ and $N_{pf}=3$ calculations. In the calculation with N_{pf} up to 3 an additional $K^\pi=0^+$ band of $N_{pf}=2$ character at low spin appears near 1 MeV and becomes yrare near $J^\pi\sim 10\hbar$.

states. When the basis is extended beyond $N_{pf}=1$, one finds new bands which appear at higher excitation energies. The lowest of these is a new excited $K=0^+$ band at ~ 1 MeV, very close in energy to the $K=0_2^+$ band in the $N_{pf}=1$ calculation. This is indicated in Fig. 6. Moreover, in some cases (^{230}U,^{238,240}Pu), this $N_{pf}=2$ band is the $K=0_2^+$ band. As seen in the figure, the $K=0_2^+$ band can have either $N_{pf}=0$ or $N_{pf}=2$ character, depending on the detailed parametrization of the Hamiltonian. They are so close in energy that a small change in the parameters will produce their inversion in excitation energy.

These two $K=0^+$ bands can be distinguished by their decay patterns, which are very different. The Hamiltonian conserves separately the number of positive (sd) and negative (pf) parity bosons. Hence, the states with $N_{pf}=0$ are not affected by extending the basis and the new states that have $N_{pf}=2$ components appear, and there is no interaction between them. The $E2$ operator of Eq. (3) will give no strength for the transitions between the positive parity states based on the $N_{pf}=2$ configuration and the positive parity states with $N_{pf}=0$ and, consequently, for the new band $B(E2;2^+_{0_{pf}}\rightarrow 4_1^+)/B(E2;2^+_{0_{pf}}\rightarrow 0_1^+)=0$. Certainly, a simple interaction which mixes the positive parity states with different pf components will induce nonzero $E2$ transition strength. A dipole-dipole interaction is an example of such a term [20]. Using the same strength for this interaction as the one used in Ref. [5] to explain the data in the transitional Ra nuclei (i.e., 0.0005 MeV), nonzero values for this ratio are obtained (see Fig. 6). The interaction is sufficiently small so that the properties of the positive parity states based primarily on $N_{pf}=0$ components remain unchanged. In fact all predictions obtained with $N_{pf}=1$ calculations remain practically unchanged by extending the basis to allow more negative parity bosons ($N_{pf}=3$). The changes are illustrated by the dashed lines in Figs. 7 and 10. Similarly in Fig. 9, the presence of more complex configurations ($N_{pf}>1$) does not modify the $E1$ strength distribution.

As was mentioned in Ref. [5], the $K=0^+$ band composed of $N_{pf}=2$ has a different moment of inertia than those composed of $N_{pf}=0$. This is illustrated in Fig. 11 where the experimental spectrum of ^{232}U is compared with the $N_{pf}=1$ and $N_{pf}=3$ calculations. In the calculation with N_{pf} up to 3 an additional $K^\pi=0^+$ band of $N_{pf}=2$ character at low spin appears near 1 MeV and becomes yrare near $J^\pi \sim 10\hbar$.

It is worth noting that the cases when $\epsilon_p \cong \epsilon_f$, i.e., ^{230,232,234}U and ^{244}Pu, are very close to the $\mathrm{SU}_{spdf}(3)$ dynamical symmetry [20] similar to ^{226}Ra discussed in Ref. [5]. The Hamiltonian for this rotational limit is

$$H=\epsilon_- \hat{N}_- - \kappa \hat{Q}^2_{spdf}. \tag{6}$$

Here $\epsilon_-=\epsilon_p=\epsilon_f$, $\hat{N}_-=\hat{n}_p+\hat{n}_f$, and $\hat{Q}_{spdf}$ is the quadrupole operator of $\mathrm{SU}_{spdf}(3)$ [see Eq. (2)]. This Hamiltonian is similar to that used in the fits presented in Sec. II [Eq. (1)] with the notable exception that in our study, $\epsilon_d \hat{n}_d$ breaks the $\mathrm{SU}_{sd}(3)$ limit, while retaining the rotational symmetry for the negative parity states.

V. CONCLUSIONS

We obtained a consistent picture over the entire nuclear region of the deformed actinides using a simple Hamiltonian in the $spdf$ space of the IBM. The structure of the low-lying states is found to have at most $N_{pf}=1$, which is equivalent to the lack of ground state dipole-octupole deformation. However, the existence of a low-lying $K=0^+$ state could indicate the presence of double octupole/dipole states. Octupole deformation is not a necessary consequence of the experimental systematics in this region.

ACKNOWLEDGMENT

Work supported by the USDOE by Grants Nos. DE-FG02-91ER-40609 and DE-FG02-88ER-40417.

[1] W. Nazarewicz, P. Olanders, I. Ragnarsson, J. Dudek, G.A. Leander, P. Möller, and E. Ruchowska, Nucl. Phys. **A429**, 269 (1984).
[2] For a review, see, P.A. Butler and W. Nazarewicz, Rev. Mod. Phys. **68**, 349 (1996).
[3] See, for example, A. Tsvetkov, J. Kvasil, and R.G. Nazmitdinov, J. Phys. G **28**, 2187 (2002), and references therein.
[4] F. Iachello and A. Arima, *The Interacting Boson Model* (Cambridge University Press, Cambridge, 1987).
[5] N.V. Zamfir and D. Kusnezov, Phys. Rev. C **63**, 054306 (2001).
[6] D. Kusnezov and F. Iachello, Phys. Lett. B **209**, 420 (1988).
[7] Y.A. Akovali, Nucl. Data Sheets **69**, 155 (1993).
[8] M.R. Schmorak, Nucl. Data Sheets **63**, 139 (1991).
[9] Y.A. Akovali, Nucl. Data Sheets **71**, 181 (1994).
[10] E.N. Shurshikov, Nucl. Data Sheets **53**, 601 (1988).
[11] E.N. Shurshikov and N.V. Timofeeva, Nucl. Data Sheets **59**, 947 (1990).
[12] Y.A. Akovali, Nucl. Data Sheets **96**, 177 (2002).
[13] E.N. Shurshikov, Nucl. Data Sheets **49**, 785 (1986).
[14] B. Ackermann *et al.*, Nucl. Phys. **A559**, 61 (1993).
[15] F.K. McGowan and W.T. Milner, Nucl. Phys. **A571**, 569 (1994).
[16] D. Ward *et al.*, Nucl. Phys. **A600**, 88 (1996).
[17] H. Baltzer *et al.*, Z. Phys. A **356**, 13 (1996).
[18] I. Wiedenhöver *et al.*, Phys. Rev. Lett. **83**, 2143 (1999).
[19] J.M. Hoogduin *et al.*, Phys. Lett. B **384**, 43 (1996).
[20] Dimitri Kusnezov, J. Phys. A **22**, 4271 (1989); **23**, 5673 (1990).
[21] A.F. Barfield, B.R. Barrett, J.L. Wood, and O. Scholten, Ann. Phys. (N.Y.) **182**, 344 (1988).
[22] P.D. Cottle and N.V. Zamfir, Phys. Rev. C **54**, 176 (1996); **58**, 1500 (1998).

[23] Dimitri Kusnezov, computer code OCTUPOLE, available upon request.
[24] D.S. Brenner, N.V. Zamfir, and R.F. Casten, Phys. Rev. C **50**, 490 (1994).
[25] R.K. Sheline and M.A. Riley, Phys. Rev. C **61**, 057301 (2000).
[26] Z. Gacsi, M. Csatlos, A. Krasznahorkay, D. Sohler, J. Gulyas, J. Timor, M. Hunyadi, J.L. Weil, and J. van Klinken, Phys. Rev. C **64**, 047303 (2001).